High contrast $GeTe_4$ waveguides for mid-infrared biomedical sensing applications

Vinita Mittal, James S. Wilkinson and Ganapathy Senthil Murugan
Optoelectronics Research Centre, University of Southampton, Southampton, SO17 1BJ
United Kingdom

ABSTRACT

Realization of single-mode waveguides is essential for ultra-sensitive biosensing in the mid-infrared molecular "fingerprint" region for biomedical lab-on-chip applications. High contrast ($\Delta n \approx 1$) germanium telluride ($GeTe_4$) single mode rib waveguides were fabricated on zinc selenide (ZnSe) substrates for evanescent field based sensing to detect analytes at low concentration. Amorphous $GeTe_4$ thin films were deposited by RF-sputtering and were found to transmit over the spectral range from 2µm - 20µm. Photolithography followed by reactive ion etching was carried out to etch the film, forming rib waveguide structures with minimum surface roughness and vertical sidewalls. It was found that films deposited at room temperature have average roughness of about 5nm. Optical constants were determined by IR-VASE ellipsometry.

Keywords: single-mode, high contrast, waveguides, evanescent field, mid-infrared, biosensing, QCL

INTRODUCTION

The mid infra-red (Mid-IR) region of the electromagnetic spectrum has a wavelength range from 3-25µm, corresponding to wavenumbers from 3333-400 cm^{-1} and the frequency range 100-12 THz. It covers an important region for a broad range of applications in various fields such as spectroscopy, pharmaceuticals, forensic, security and safeguard, astronomy, climate and pollution monitoring, sensing and detection of some prominent gases, liquids and solids [1,2]. These applications are not only technologically significant but also will contribute to a safe and secure society. The present work is focused on developing waveguides and integrated optical devices for evanescent field based sensing in the mid-infrared region for biomedical applications. There is a need for label-free biosensing which can provide accurate and reliable information rapidly and at low cost. Since fundamental molecular vibrations occur mainly in the mid-IR spectral region from 2 to 13 µm, analytes of very low concentration can be detected using their fingerprint absorption in this region, offering high selectivity over a wide range of compounds without labelling. Optical approaches are the most widely used for chemical analysis in microsystems as they have an excellent track-record in chemical analysis, usually show the lowest limits of detection and provide the greatest chemical or morphological information on the analyte. The presence of biological markers of disease or of molecular changes in clinical samples can be distinguished by studying their mid-IR spectra, leading to the rapid identification and diagnosis of diseases at point-of-care.

The success of VIS/NIR technologies has motivated researchers to work vigorously towards evolving mid-infrared technology. Many important breakthroughs have been achieved in the last few decades, such as the development of the quantum cascade laser (QCL) in 1994 [3], and these have renewed interest in mid-IR technology because of wide tunability, high power, compact design and simple operation. Fabrication of devices to work at mid-IR wavelengths are, in principle, easier as the fabrication tolerances for defects, roughness and feature dimensions also increase with longer wavelengths [4]. Integrated devices for mid-IR biosensing in a "lab on a chip" need waveguides for efficient and reproducible interaction of analyte with photons. Since commonly used silicate glasses do not transmit at wavelengths beyond 3µm and some mid-IR transmitting glasses such as the fluoride glasses degrade when in contact with water, novel materials need to be explored and engineered for specific mid-IR applications. Chalcogenides are considered the most advanced potential materials for infrared technology for their 1) transparency in infrared region, 2) photosensitivity, 3) easy processability in different compositions and geometries, and 4) high refractive index for better optical confinement and enhanced optical intensities [5]. Recently chalcogenide waveguides of $Ge_{11.5}As_{24}Se_{64.5}$ with an

index contrast of 0.4 were designed to work in the spectral range from 2.5µm to 6.6µm and losses at several wavelengths were studied [6]. We have chosen a tellurium-rich germanium telluride compound; $Ge_{20}Te_{80}$ or $GeTe_4$ for its broad IR transparency in the region of 2 µm - 20µm and high refractive index of 3.3 at 10.0µm. A range of chalcogenide compositions have been explored for phase change memory devices [7] and crystalline $GeTe_4$ was reported to be a promising phase change memory material due to its good thermal stability and low power consumption [8]. Recently $GeTe_4$ rib waveguides were explored in the mid-IR range of 6-20 µm for spatial interferometry in the search for earth-like planets, where the index contrast between the $GeTe_4$ core and the $Te_{75}Ge_{15}Ga_{10}$ substrate was about 4×10^{-2} [9-11]. In this paper, we describe the fabrication of a "high contrast" ($\Delta n \approx 1$), $GeTe_4$ single mode rib waveguide on a ZnSe substrate, transmitting over the spectral range from 2µm - 20µm. A high index contrast allows realization of single mode waveguides with smaller cross-sections, and hence compact designs, and also enables strong optical intensities at the surface of the waveguides for high-sensitivity evanescent spectroscopy. In this paper, we present the results of deposition of $GeTe_4$ glass thin films and their characterization for structural and optical properties and the fabrication of rib waveguides in these films by photolithography and dry etching.

EXPERIMENTAL PROCEDURES

$GeTe_4$ films were deposited on 2 mm thick polycrystalline ZnSe substrate by RF magnetron sputtering in an argon atmosphere. A commercial target of germanium telluride (150mm diameter x 6mm thick) with a Ge:Te molar ratio of 1:4 with 99.99% purity was used. The distance between the substrate and the target was fixed at 80mm. The base pressure of the system was 7.5×10^{-7}Torr before deposition. Most of the deposition was carried out with the substrate maintained at room temperature although substrate could gain some temperature due to the bombardment of sputtering species on the surface. Several films were deposited at different temperatures to study the effect of deposition temperature on film properties. Deposition parameters such as sputtering pressure, power, and argon flow rate were varied to optimize the deposition conditions and to study their effect on the resulting films. The thickness of the films was measured using a KLA Tencor stylus profilometer. The phase of the deposited films was determined by using a Rigaku X-ray Diffraction system. A Zeiss Scanning electron microscopy (SEM) and a Veeco atomic force microscopy (AFM) were used to observe the film surface morphology and roughness. A Thermoscientific X-ray photoelectron spectroscopy (XPS) was used to determine the composition of the film. An Agilent Technologies Fourier transform infrared (FTIR) spectroscopy was used to measure the transmission spectrum of the films. The refractive index of the deposited films was measured through ellipsometry using a Woollam Co., Inc. IR-VASE (Woollam Co., Inc.) system. Standard photolithography followed by a Plasmalabs reactive ion etcher (RIE) was used to fabricate the waveguides in the films by creating rib structures. A Thermoscientific waterless polishing system that used ethanediol as a solvent was used to polish the end facets of the waveguides.

RESULTS AND DISCUSSION

The sputtering power and pressure were varied to optimize the deposition rate. Figure1 and 2 show the relationship of deposition rate to sputtering pressure and power, respectively, for $GeTe_4$ films deposited on ZnSe substrate. The sputtering pressure was varied from 3sccm to 30sccm at a fixed power of 50W and an Ar flow rate of 20sccm. A plasma was not supported at pressures below 3mT and above 30mT, so the optimization process for the deposition rate was performed in the range of 5-25mT. It is seen that deposition rate decreases with sputtering pressure. Pressure of 10-15mT was chosen to be optimum pressure that resulted in a deposition rate of 0.6-0.7µm/h. Sputtering power was varied from 30W to 60W at a fixed sputtering pressure of 10mT and a fixed Ar flow rate of 25sccm. At a fixed pressure, with increasing power, the sputtering yield increases and hence the deposition rate increases [12].

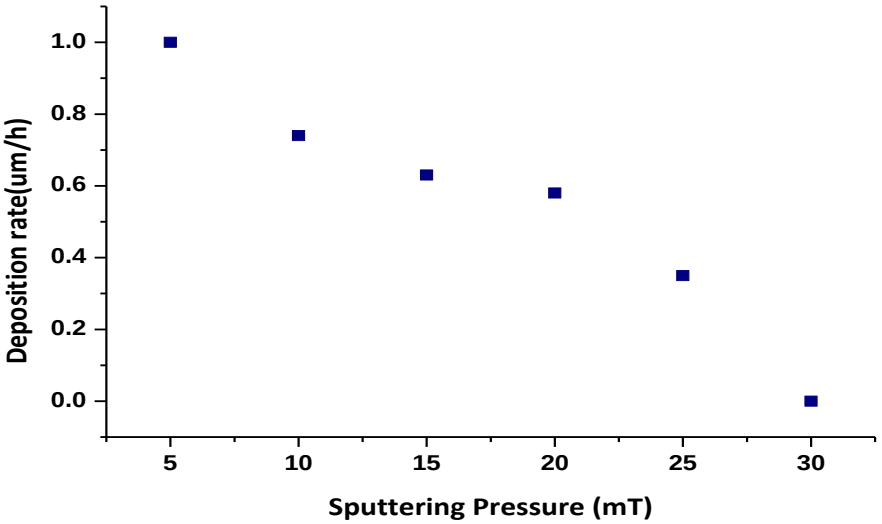

Figure1 The deposition rate of GeTe films on ZnSe substrates as a function of sputtering pressure at a fixed sputtering power of 50W and Ar flow rate of 20sccm.

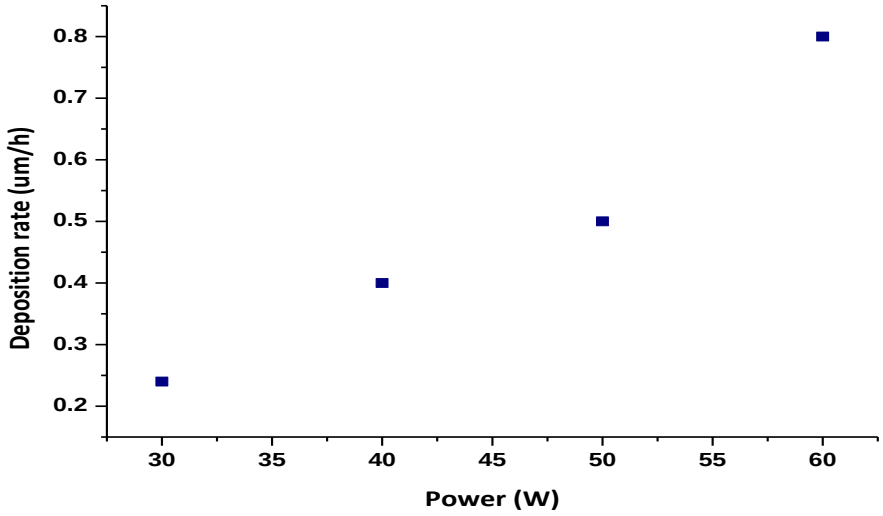

Figure2 The deposition rate of $GeTe_4$ films on ZnSe substrates as a function of sputtering power at a fixed sputtering pressure of 10mT and Ar flow rate of 25sccm.

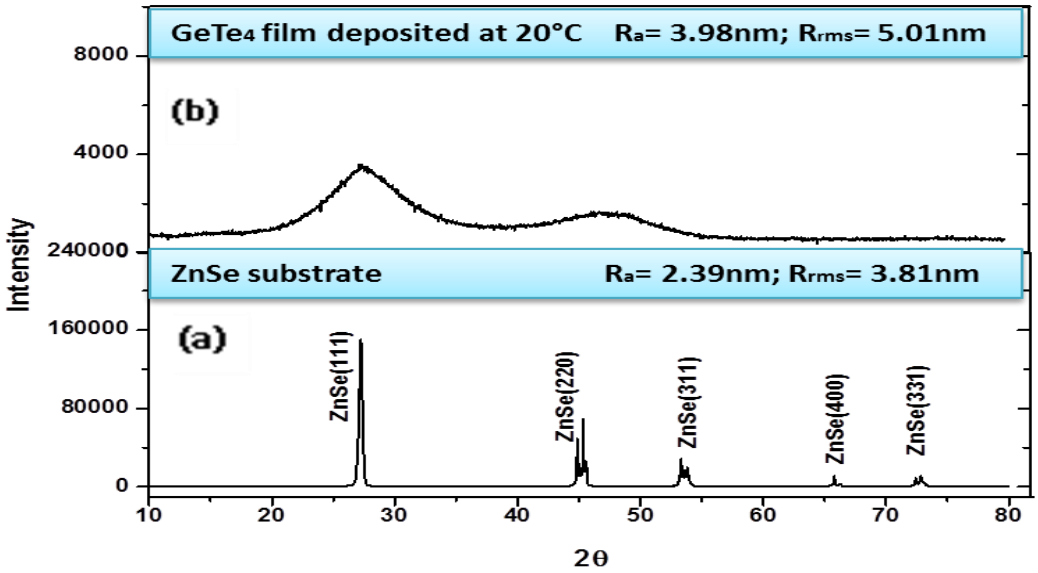

Figure3 XRD spectra and average and rms roughness values from AFM measurements for a 1square micron scan area of (a) a ZnSe substrate and (b) a $GeTe_4$ film deposited at 20°C .

Figure 3(a) depicts the XRD pattern for the ZnSe substrate. Sharp peaks in different planes of the material confirm its polycrystalline nature. The average (R_a) and root mean square (R_{rms}) roughness values for ZnSe substrate are also reported in the same image and are 2.39nm and 3.81nm respectively. Similarly, figure 3 (b) depicts the XRD pattern for $GeTe_4$ film. The broad curve with the absence of any sharp peaks in any particular plane confirms that the deposited films are amorphous in nature. The films remain amorphous at different sputtering powers (tested for 30W to 60W) and deposition temperatures (20°C to 250°C). R_a and R_{rms} values for the $GeTe_4$ film deposited at 20°C is 3.98 nm and 5.01nm respectively. Although this value of roughness is insignificant for our device and application in the Mid-infrared wavelengths, we found that this roughness value can be further reduced to below 2nm when the films are deposited at higher temperatures. Figure 4a shows an SEM image of the top surface of a deposited $GeTe_4$ film which shows that the surface of the film is not entirely smooth. It has a few defects that are mainly because of defects in substrate preparation. However, the surface roughness is well below the permissible range as discussed above. Figure4 b) shows cross-section of a 2µm thick $GeTe_4$ film deposited on ZnSe. The film looks dense and free from any columnar structures. Since the substrate is polycrystalline, its different planes are also visible in the SEM image.

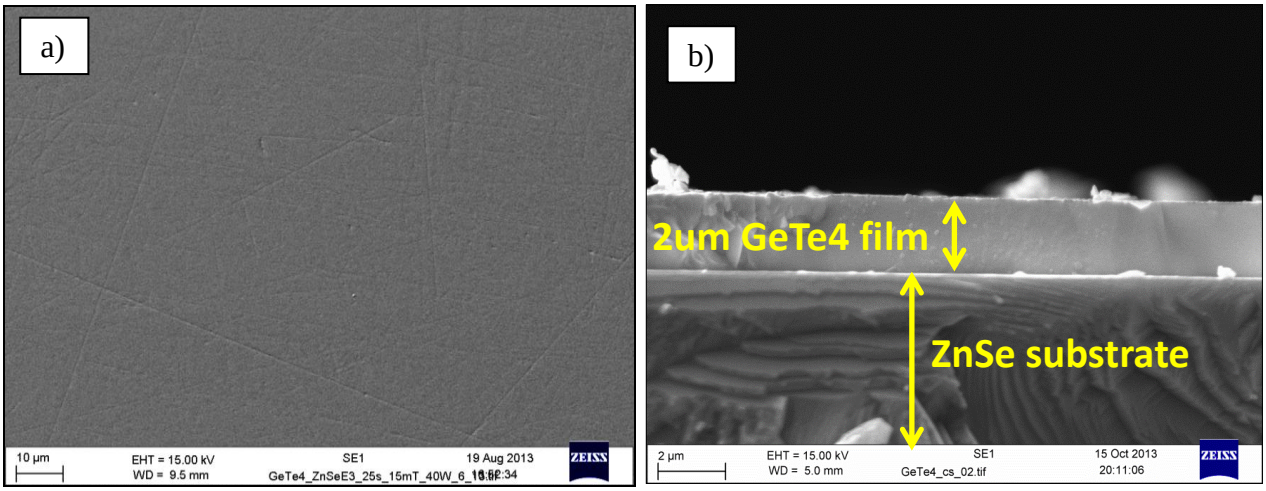

Figure4 SEM images of a) surface and b) cross-section of a $GeTe_4$ film deposited on ZnSe.

The deposited $GeTe_4$ films were characterized by FTIR and found to transmit over the full spectral range from 2µm - 20µm as shown in Figure5. The transmission of ZnSe was first obtained as a background spectrum. It was then subtracted to correct the transmission spectrum for the $GeTe_4$ films. The transmission of the ZnSe substrate is also shown in figure 5 for the same wavelength range.

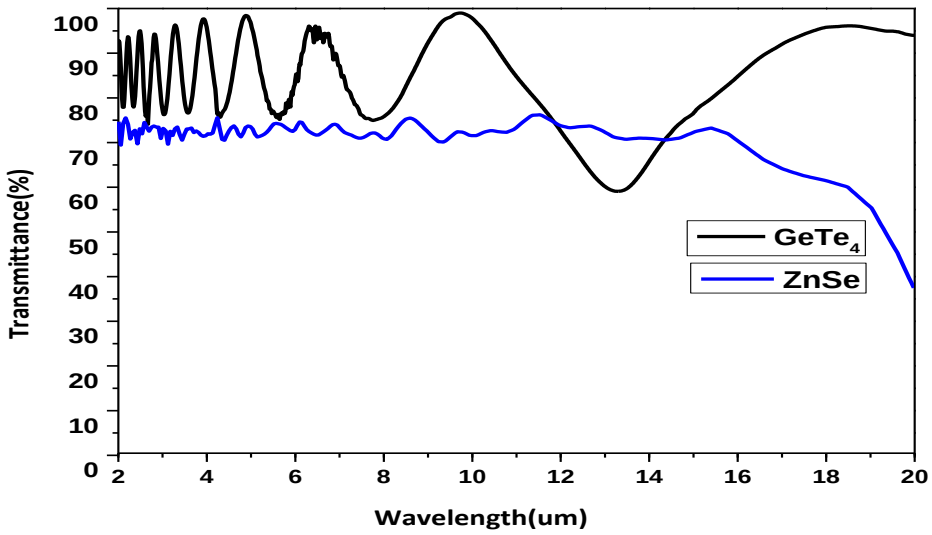

Figure 5 Transmission spectra of the $GeTe_4$ film and the ZnSe substrate as measured by FTIR.

The refractive index and extinction coefficient for the substrate and the film were determined by ellipsometry for the wavelength range from 2-30µm as shown in Figures 6 and 7. There is a strong absorption peak observed in the 11-16µm region corresponding to a Ge-O stretching vibration [13,14]. This is due to oxygen contamination in the film as confirmed by XPS depth profile analysis (Figure8). Here the XPS spectrum was measured after every 1minute of etching the film surface until the substrate was visible. So every minute corresponds to approximately 40nm etch depth. It was found that the top 40nm surface layer is comprised of oxides in the form of GeO and TeO_2. A more detailed analysis showed that TeO_2 is present in the first few nm (10nm) of the film whereas about 2% GeO was present throughout the film. It is expected that the bulk oxide contamination could be eliminated by further purifying the target material before target fabrication and that the surface contamination could be eliminated by depositing a passivation layer on the surface of the deposited films before removing from the sputtering chamber.

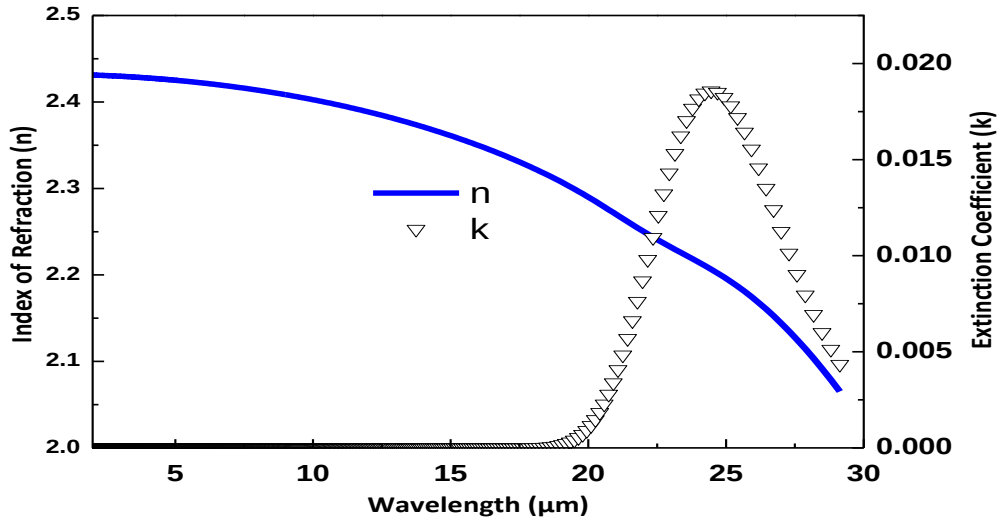

Figure6 Optical constants n and k for the ZnSe substrate determined by ellipsometry.

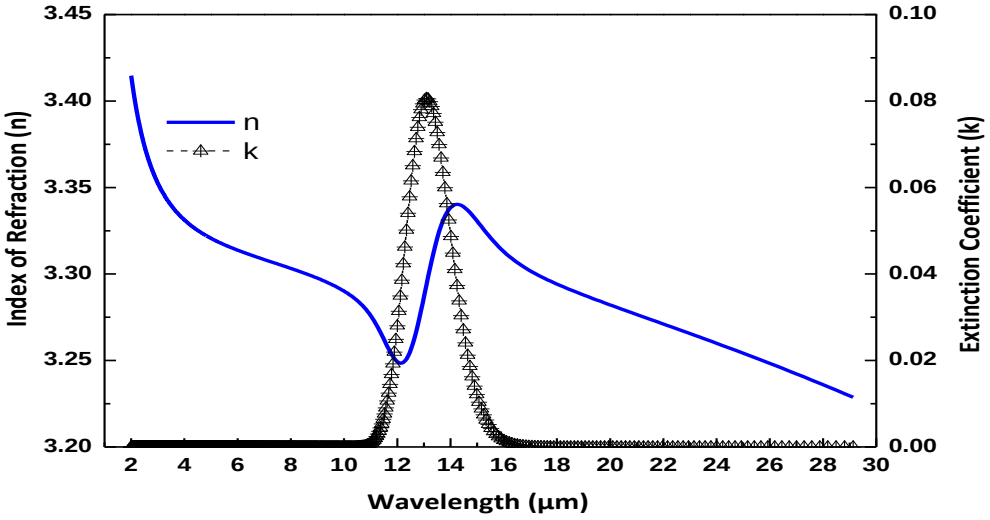

Figure7 Optical constants n and k for the $GeTe_4$ film determined by ellipsometry.

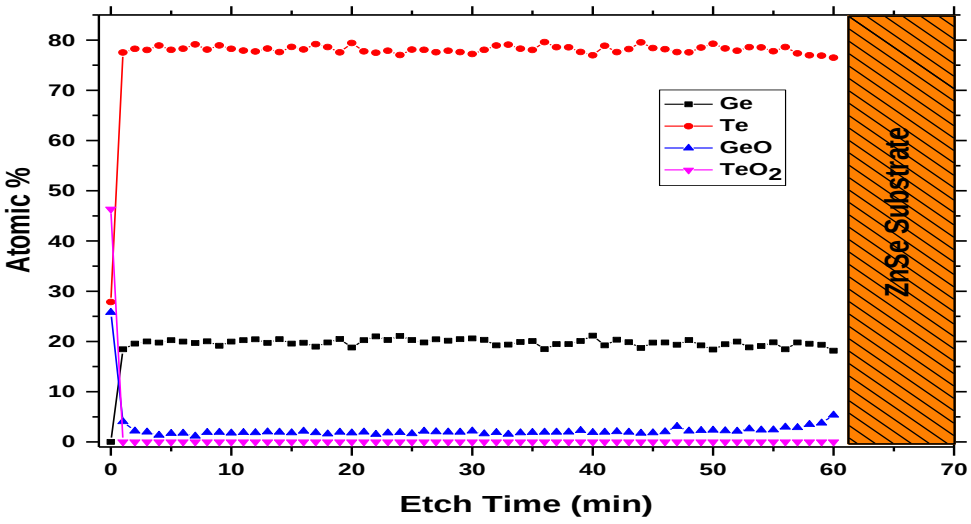

Figure8 Concentration depth profile of a $GeTe_4$ film by XPS.

The material losses in dB/cm were calculated over the wavelength range from 2 to 29μm from extinction coefficient taken from the ellipsometry data, and are shown in Figure 9. It can be clearly seen that the material losses are less than 0.1 dB/cm for wavelengths below 10μm, which is very promising for the spectroscopy of many clinical analytes. Beyond this wavelength, the losses began to increase leading to very high losses in 11-16μm region, as shown in the inset. These losses are primarily due to the presence of oxides, which can be minimized by using purer materials and by modifying fabrication techniques.

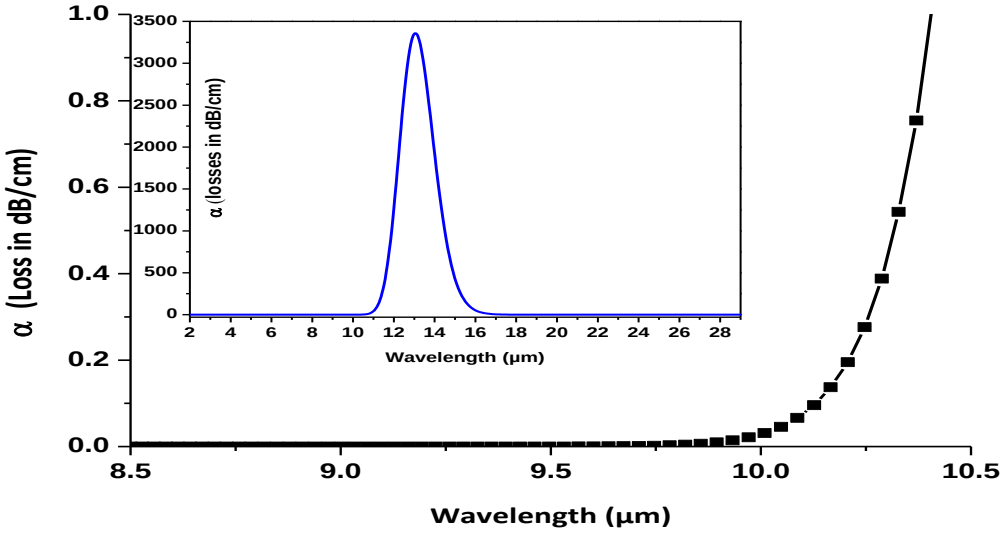

Figure 9 Losses in dB/cm calculated from extinction coefficient for $GeTe_4$ film at wavelengths below 10.5μm (inset: loss in dB/cm for the wavelength range of 2-29μm)

Photolithography followed by reactive-ion etching was carried out to pattern the film into rib structures with the aim of achieving low surface roughness and vertical sidewalls. S1813 photoresist was spun onto the film using resist spinner and soft-baked for 30min at 90°C in an oven. A photolithographic mask with channel waveguide stripe patterns of

various widths and separations was used to pattern the film. After developing the resist, samples were hard-baked for 30 min at 120°C in an oven. An optimized mixture of CHF_3:O_2 was used to etch the films into rib structures. It was found that the selectivity of the optimized mixture was 1:1. Rib structures with different dimensions and etch depths were fabricated. Soref's condition was applied to find the rib etch depth and width, which states that for any rib structures to be single moded, its etch depth should be half or less than half of the total film thickness [15,16]. In this paper, we will discuss rib structures with an etch depth of 200 nm and width 4.5 µm on 1.75µm thick film of $GeTe_4$ on ZnSe, as shown in Figure10.

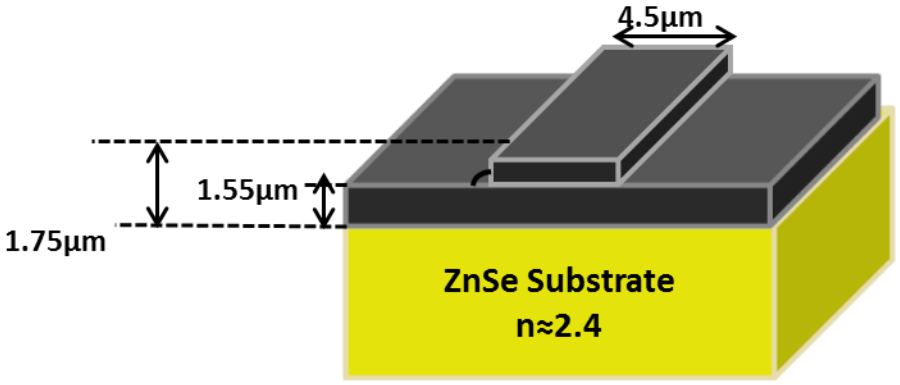

Figure10 $GeTe_4$ rib waveguide fabricated on ZnSe

It was predicted that for this geometry, the waveguide will support fundamental TE and TM modes for the wavelengths from 7-10µm. The predicted effective indices, N_{eff}, for the TE_{00} and TM_{00} modes as calculated by effective index method at different wavelengths [17] for the above geometry are tabulated in Table 1.

Table 1 Predicted N_{eff} of TE_{00} and TM_{00} modes for the rib waveguide structure shown in Fig. 10.

Wavelength (µm)	Neff 2-D effective index approximation, TE 00 mode	Neff 2-D effective index approximation, TM 00 mode
7.0	2.97	2.80
8.0	2.91	2.70
9.0	2.85	2.61
10.0	2.80	2.53

For end face coupling, polishing of the input and output faces of the waveguides was required which was obtained by waterless polishing using alumina particles mixed in ethane diol. Water was avoided throughout the fabrication process as it can produce H_2Se gas when in contact with ZnSe. Also $GeTe_4$ films have a tendency to form an oxide layer when in contact with water.

Mode intensity profile measurements are presently underway using light from a Block Engineering Inc. QCL coupled into the waveguide using a ZnSe microscope objective lens. The QCL is tunable from 6-12 µm with an average output power of about 100mW and beam diameter of about 3mm. A ZnSe objective lens is used to focus the light onto the waveguide input end facet with a spot size of approximately 20 µm at 8µm wavelength. The transmitted light from the output end face of the waveguide is then collected by another ZnSe objective lens to be measured by a power meter or imaged by a Xenics mid-IR camera.

CONCLUSION

High-contrast germanium telluride slab and rib waveguides were fabricated on zinc selenide substrates for mid-infrared biosensing applications. The 2µm thick films, deposited by RF sputtering at a rate of approximately 0.5 µm per hour, were found to transmit over the spectral range from 2µm - 20µm. The average surface roughness of the films was found to be 5nm or less, sufficiently low for low-loss waveguides at mid-IR wavelengths. The deposited films were amorphous as confirmed by XRD, as required to minimize volume scattering. XPS analysis showed the presence of some oxygen contamination in the film which is primarily due to the Ge-O absorption at 12-15µm. This contamination resulted in large losses at wavelengths longer than 10µm, as determined by spectroscopic ellipsometry. The low material losses at wavelengths below 10µm show great promise for sensing applications for a wide range of clinical analytes. Further improvements in the material purity are expected to lead to waveguides for the full spectral region between 2µm and 16µm. Rib waveguides with minimum surface roughness and vertical sidewalls were realized by reactive ion etching and are presently being characterized for loss and modal intensity distribution.

ACKNOWLEDGEMENTS

This research was funded by the European Research Council under the European Union's Seventh Framework Programme (FP7/2007 -2013) ERC grant agreement no. 291216 Wideband Integrated Photonics for Accessible Biomedical Diagnostics. We would like to acknowledge Neil Sessions, Mike Perry and Owain Clark for the support they provided in the cleanroom. We would also like to thank Feras Al Saab for his help in carrying out XRD and Dr. Harold Chong and Dr. David Payne for providing training in AFM.

REFERENCES

[1] A. B. Seddon: A prospective for new Mid-infrared medical endoscopy using chalcogenide glasses, International Journal of Applied Glass Science, Vol. 2(3), pp. 177, 2011

[2] A. Rodenas, G. Martin, B. Arezki, N. Psaila, G. Jose, A. Jha, L. Labadie, P. Kern, A. Kar and R. Thomson: Three-dimensional mid-infrared photonics circuits in chalcogenide glass, Optics Letters, Vol. 37(3), pp.392, 2012

[3] J. Faist, F. Capasso, D.L. Sivo, C. Sirtori, A.L. Hutchinson, A.Y. Cho, Quantum Cascade laser, Science, 264, 553-556, 1994

[4] B. Mizaikoff: Waveguide-enhanced mid-infrared chem/bio sensors, RSC publication, The Royal Society of Chemistry, Chem. Soc. Rev., 2013

[5] V. G. Ta'eed, N. J. Baker, L. Fu, K. Finsterbusch, M. R. E. Lamont, D. J. Moss, H. C. Nguyen, B. J. Eggleton, D. Y. Choi, S. Madden and B. L. Davies: Ultrafast all-optical chalcogenide glass photonic circuits, Optics Express, Vol. 15(15), pp. 9205, 2007

[6] P Ma, D-Y Choi, Y Yu, X Gai, Z Yang, S Debarma, S Madden, B L Davies, 'Low-loss chalcogenides waveguides for chemical sensing in the mid-infrared, Optics Express, Vol 21 (24), pp. 29927, 2013

[7] H. Cheng, C. Jong, C. Lee, T. Chin: Wet-etching characteristics of Ge2Sb2Te5 thin films for phase change memory, IEEE transactions on magnetics, Vo.l 41(2), pp. 1031, 2005

[8] L. Run, T. Shi-Yu, B. Gang, Y. Qiao-Nan, L. Xue-Xin, X. Yi-Dong, Y. Jiang and L. Zhi-Guo: $GeTe_4$ as a candidate for phase change memory application, Chin. Phys. Lett., Vol. 30(5), pp. 058101, 2013

[9] C. Vigreux, E. Barthelemy, L. Bastard, J-E. Broquin, M. Barillot, S. Menard, G. Parent and A. Pradel: Realization of single-mode telluride rib waveguides for mid-IR applications between 10 and 20µm, Optics Letters, Vol. 36(15), pp.2922, 2011

[10] C. Vigreux, A. Pradel, L. Bastard, J-E. Broquin, G. Parent¸X Zhang and M. Barillot: All-Telluride Waveguides for Nulling Interferometry in 6-20 µm Spectral Range: fabrication and Testing, ICTON 2011

[11] C. Vigreux, M. Barillot, E. Barthelemy, L. Bastard, J-E. Broquin, V. Kirschner, S. Menard, G. Parent, C Poinsot, A. Pradel, S. Zhang, and X. Zhang: All-telluride channel waveguides for mid-infrared applications: OSA/AIOM 2011

[12] B.L. Zhu, J. Wang, S.J. Zhu, J. Wu, D.W. Zeng and C. S. Xie: Optimization of sputtering parameters for deposition of Al-doped ZnO films by rf magnetron sputtering in Ar +H2 ambient at room temperature, Thin Solid Films Vol. 520, pp. 6963, 2012
[13] C. Vigreux, E. Bonhomme, A. Pradel: Te-rich Ge-As-Se_Te bulk glasses and films for future IR-integrated optics, J. non-Crys. Solids, Vol. 353, pp. 1388, 2007
[14] X. H. Zhang, L. Calvez, V. Seznec, H. L. Ma, S. Danto, P. Houizot, C. Boussard-Pledel, J. Lucas: Infrared transmitting glasses and glass-ceramics, J. non-Crys. Solids, Vol. 352, pp. 2411, 2006
[15] R.A. Soref, J. Schmidtchen and K. Peterman: Large single mode rib waveguides in GeSi-Si and Si-on SiO_2, IEEE Journal of Quantum Electronics, Vol. 27 (8), 1991
[16] K.Petermann: Properties of optical Rib-Guides with large cross-section, Ubertragungstechnik. Electronics and communication, Vol. 30, pp. 139-140, 1976
[17] http://www.computational-photonics.eu/eims.html